

## SUPPLEMENTAL DATA

### **An ATP-competitive mTOR inhibitor reveals rapamycin-resistant functions of mTORC1**

Carson C. Thoreen, Seong A. Kang, Jae Won Chang, Qingsong Liu, Jianming Zhang, Yi Gao, Laurie J. Reichling, David M. Sabatini, and Nathanael S. Gray

### **Supplemental Experimental Procedures**

#### *PI3K Invitrogen Adapta Assays*

For lipid kinase assays, 10  $\mu$ L reactions were performed in triplicate with variable amounts of inhibitor with 10  $\mu$ M ATP, 2 mM DTT, and a kinase-specific buffer and substrate. 50  $\mu$ M PIP2:PS lipid kinase substrate was used for p110 $\alpha$ /p85 $\alpha$ , p110 $\beta$ /p85 $\alpha$  and p110 $\gamma$ . 100  $\mu$ M PIP2:PS lipid kinase substrate was used for p110 $\delta$ /p85 $\alpha$ . 100  $\mu$ M PI lipid kinase substrate was used for PI3K-C2 $\alpha$  and PI3K-C2 $\beta$ . 100  $\mu$ M PI:PS lipid kinase substrate was used for hVPS34. The buffer for p110 $\delta$ /p58 $\alpha$ , p110 $\beta$ /p85 $\alpha$ , p110 $\delta$ /p85 $\alpha$ , PI3K-C2 $\alpha$ , and PI3K-C2 $\beta$  was 50 mM Hepes pH 7.5, 3 mM MgCl<sub>2</sub>, 1 mM EGTA, 100 mM NaCl, and 0.03% CHAPS. The buffer for hVPS34 was 50 mM Hepes pH 7.3, 0.1% CHAPS, 1 mM EGTA, and 5 mM MnCl<sub>2</sub>. The enzyme concentrations were 0.12, 4.5, 0.79, 3.5, 6.3, 42, and 2.8 nM for p110 $\alpha$ /p85 $\alpha$ , p110 $\beta$ /p85 $\alpha$ , p110 $\delta$ /p58 $\alpha$ , p110 $\gamma$ , PI3K-C2 $\alpha$ , PI3K-C2 $\beta$ , and hVPS34, respectively. After 1 hour at room temperature, 5  $\mu$ L of detection mix was added, comprised of 12 nM Alexa Fluor647<sup>®</sup> ADP Tracer, 6 nM Adapta<sup>™</sup> Eu-anti-ADP Antibody, 20 mM Tris pH 7.5, 0.01% NP-40, and 30 mM EDTA. After 30 minutes, the plates were read on a Tecan InfiniTE<sup>®</sup> F500 or BMG PHERAstar plate reader. Instrument settings suitable for Adapta<sup>™</sup> assays were used measuring emission at 665 and 615 nm after excitation at 340 nm with a lag time of 100  $\mu$ s and integration time of 200  $\mu$ s. The raw emission ratio (emission at 665 nm  $\div$  emission at 615 nm) values were converted to product formation (% conversion of ATP) using nucleotide (ATP:ADP) standard curves. IC<sub>50</sub> values were calculated from plots of compound concentration versus product formation. mTOR enzyme assays were performed as previously described (1).

## Supplemental Figures

Kinase ID	% Ctrl	Kinase ID	% Ctrl	Kinase ID	% Ctrl
AAK1		FGFR3		PIM3	
ABL1		FGFR3(G697C)		PIP5K1A	
ABL1(E255K)		FGFR4		PIP5K2B	
ABL1(F317I)		FGR		PKAC-alpha	
ABL1(F317L)		FLT1	20	PKAC-beta	
ABL1(H396P)		FLT3		PKMYT1	
ABL1(M351T)		FLT3(D835H)		PKN1	
ABL1(Q252H)		FLT3(D835Y)		PKN2	
ABL1(T315I)	33	FLT3(ITD)		PLK1	
ABL1(Y253F)		FLT3(K663Q)	29	PLK3	
ABL2		FLT3(N841I)		PLK4	
ACVR1		FLT4		PRKCD	
ACVR1B		FRK	26	PRKCE	
ACVR2A		FYN		PRKCH	
ACVR2B		GAK		PRKCQ	
ACVRL1		GCN2(Kin.Dom.2,S808G)		PRKD1	
ADCK3	15	GSK3A		PRKD2	
ADCK4	23	GSK3B		PRKD3	
AKT1		HCK		PRKG1	
AKT2		HIPK1		PRKG2	
AKT3		IGF1R		PRKR	
ALK		IKK-alpha		PRKX	
AMPK-alpha1		IKK-beta		PTK2	
AMPK-alpha2		IKK-epsilon		PTK2B	
ANKK1		INSR		PTK6	
ARK5		INSRR		RAF1	33
AURKA		IRAK3		RET	
AURKB		ITK		RET(M918T)	
AURKC		JAK1(Kin.Dom.1)	27	RET(V804L)	
AXL		JAK1(Kin.Dom.2)		RET(V804M)	
BIKE		JAK2(Kin.Dom.2)		RIOK1	
BLK		JAK3(Kin.Dom.2)		RIOK2	
BMPR1A		JNK1	33	RIOK3	
BMPR1B		JNK2	33	RIPK1	3
BMPR2		JNK3		RIPK2	
BMX		KIT		RIPK4	
BRAF		KIT(D816V)		ROCK2	
BRAF(V600E)		KIT(V559D)		ROS1	
BRSK1		KIT(V559D,T670I)	19	RPS6KA1(Kin.Dom.1)	
BRSK2		KIT(V559D,V654A)		RPS6KA1(Kin.Dom.2)	
BTK		LATS1		RPS6KA2(Kin.Dom.1)	
CAMK1		LATS2		RPS6KA2(Kin.Dom.2)	
CAMK1D		LCK		RPS6KA3(Kin.Dom.1)	
CAMK1G		LIMK1		RPS6KA4(Kin.Dom.1)	
CAMK2A		LIMK2		RPS6KA4(Kin.Dom.2)	
CAMK2B		LKB1	15	RPS6KA5(Kin.Dom.1)	

CAMK2D		LOK	6.8	RPS6KA5(Kin.Dom.2)	
CAMK2G		LTK		RPS6KA6(Kin.Dom.1)	
CAMK4		LYN		RPS6KA6(Kin.Dom.2)	
CAMKK1		MAP3K3		SgK085	
CAMKK2		MAP3K4		SgK110	
CDC2L1		MAP3K5		SLK	
CDC2L2		MAP4K1		SNARK	
CDK11	2	MAP4K2		SNF1LK	
CDK2		MAP4K3	25	SNF1LK2	25
CDK3		MAP4K4	15	SRC	
CDK5		MAP4K5	18	SRMS	
CDK7		MAPKAPK2	10	SRPK1	
CDK8	13	MAPKAPK5	16	SRPK2	
CDK9		MARK1		SRPK3	
CDKL2		MARK2		STK16	25
CHEK1		MARK3		STK33	
CHEK2		MARK4		STK35	28
CIT		MEK1		STK36	18
CLK1		MEK2		SYK	
CLK2		MEK3		TAK1	
CLK3		MEK4		TAOK1	
CLK4		MEK6		TAOK3	
CSF1R		MELK		TEC	
CSK		MERTK		TESK1	
CSNK1A1L		MET		TGFBR1	
CSNK1D		MINK		TGFBR2	
CSNK1E		MKNK1		TIE1	
CSNK1G1		MKNK2		TIE2	25
CSNK1G2		MLCK		TLK1	
CSNK1G3		MLK1		TLK2	
CSNK2A1		MLK2		TNIK	
CSNK2A2		MLK3		TNK1	15
DAPK1		MRCKA	0.8	TNK2	
DAPK2		MRCKB	6.6	TNNI3K	
DAPK3		MST1	24	TRKA	
DCAMKL1		MST1R		TRKB	
DCAMKL2		MST2		TRKC	
DCAMKL3		MST3		TSSK1	
DDR1		MST4		TTK	30
DDR2		MUSK		TXK	
DLK		MYLK		TYK2(Kin.Dom.1)	
DMPK		MYLK2		TYK2(Kin.Dom.2)	
DMPK2	3	MYO3A		TYRO3	
DRAK1		MYO3B		ULK1	
DRAK2		NDR2		ULK2	
DYRK1B		NEK1		ULK3	
EGFR		NEK2		VEGFR2	
EGFR(E746-A750del)		NEK5	11	WEE1	
EGFR(G719C)		NEK6		WEE2	
EGFR(G719S)		NEK7		YANK2	
EGFR(L747-E749del,		NEK9		YANK3	

A750P)		NLK		YES	
EGFR(L747-S752del, P753S)				YSK1	
EGFR(L747- T751del,Sins)		p38-alpha		ZAK	23
EGFR(L858R)		p38-beta		ZAP70	
EGFR(L861Q)		p38-delta			
EGFR(S752-I759del)		p38-gamma			
EPHA1		PAK1			
EPHA2		PAK2			
EPHA3		PAK3			
EPHA4		PAK4			
EPHA5		PAK6			
EPHA6		PAK7/PAK5			
EPHA7		PCK1			
EPHA8		PCK2			
EPHB1		PCK3			
EPHB2		PDGFRA			
EPHB3		PDGFRB			
EPHB4		PDPK1			
ERBB2		PFTAIRE2			
ERBB4		PFTK1			
ERK1		PHKG1			
ERK2		PHKG2			
ERK3		PIK3C2B	26		
ERK4		PIK3CA	1.5		
ERK5	6.4	PIK3CA(E545K)	0.65		
ERK8		PIK3CB	28		
FER		PIK3CD			
FES		PIK3CG	34		
FGFR1		PIM1			
FGFR2	25	PIM2			

### Figure S1. Torin1 has negligible off-target activity against a diverse panel of kinases

Torin1 was profiled at a concentration of 10  $\mu$ M against a diverse panel of 353 kinases by Ambit Biosystems. Scores for primary screen hits are reported as a percent of the DMSO control (% Control). For kinases where no score is shown, no measurable binding was detected. The lower the score, the lower the Kd is likely to be such that scores of zero represent strong hits. Scores are related to the probability of a hit but are not strictly an affinity measurement. At a screening concentration of 10  $\mu$ M, a score of less than 10% implies that the false positive probability is less than 20% and the Kd is most likely less than 1  $\mu$ M. A score between 1- 10% implies that the false positive probability is less than 10%, though it is difficult to assign a quantitative affinity from a single-point primary screen. A score of less than 1% implies that the false positive probability is less than 5% and the Kd is most likely less than 1  $\mu$ M.

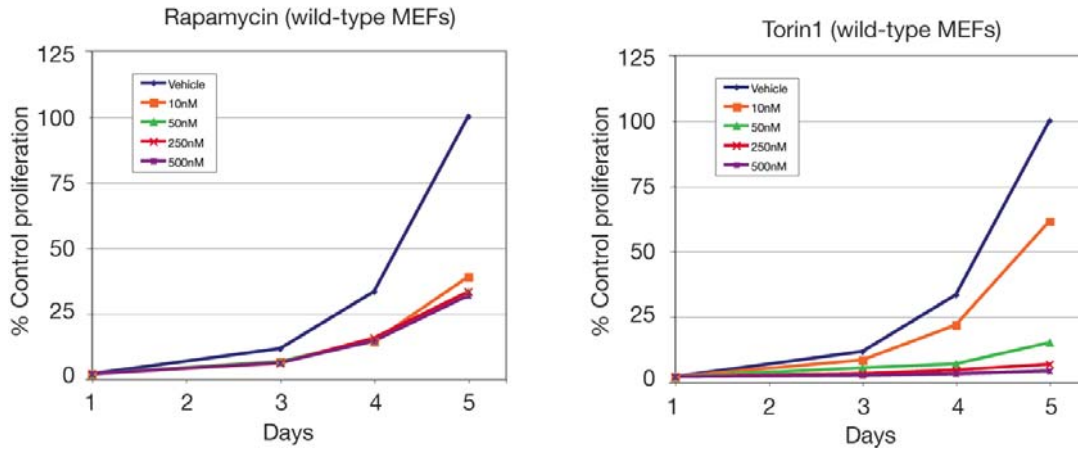


**Figure S2. Torin1 and rapamycin differentially affect cell growth at equal concentrations**

mTOR inhibition by Torin1 but not rapamycin prevents the proliferation of wild-type MEFs. MEF ( $p53^{-/-}$ ) cells were grown in the presence of vehicle, or 10 nM, 50 nM, 250 nM or 500 nM rapamycin or Torin1 for 4 days. Cell proliferation was measured in triplicate at indicated time-points using the CellTiterGlo viability assay.

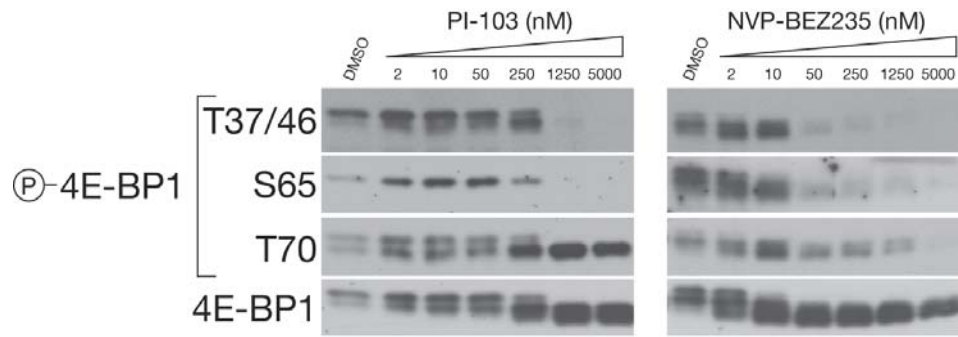


**Figure S3. Dual-mTOR/PI3K inhibitors prevent phosphorylation of Torin1-sensitive 4E-BP1 sites**

MEFs ( $p53^{-/-}$ ) were treated with increasing concentrations of the dual-mTOR/PI3K inhibitors PI-103 or BEZ-235 for 1 h and then analyzed by immunoblotting for the indicated proteins and phosphorylation states.

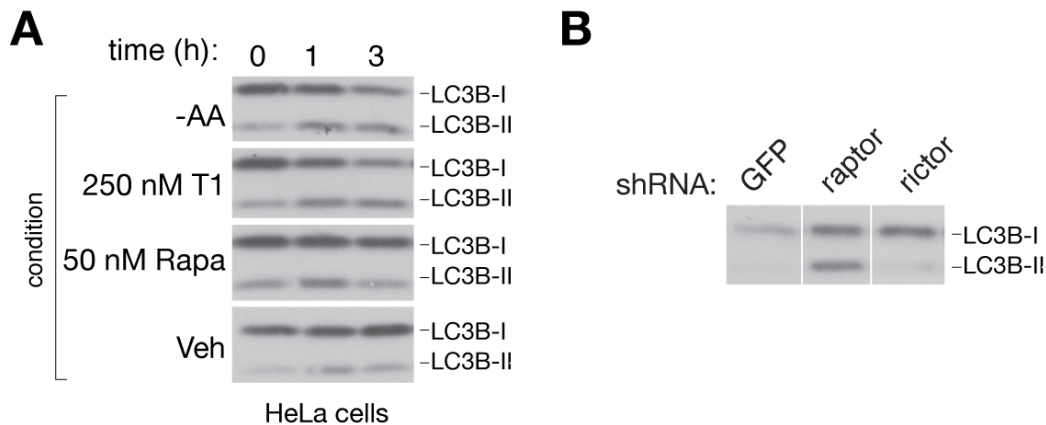


**Figure S4. mTORC1 inhibition promotes autophagy**

(A) Amino acid starvation and Torin1 induce autophagy in HeLa cells. HeLa cells were treated with vehicle (DMSO), 50 nM rapamycin, 250 nM Torin1 or grown in amino acid-free conditions for 0, 1, or 3 hours. Cells were lysed at the indicated time points and analyzed by immunoblotting.

(B) Selective inactivation of mTORC1 using RNAi promotes LC3 degradation. MEFs (p53<sup>-/-</sup>) were infected with lentivirus expressing either control, raptor- or rictor-specific shRNAs and grown for 4 days. Cell lysates were then analyzed by immunoblot using antibodies specific LC3B.

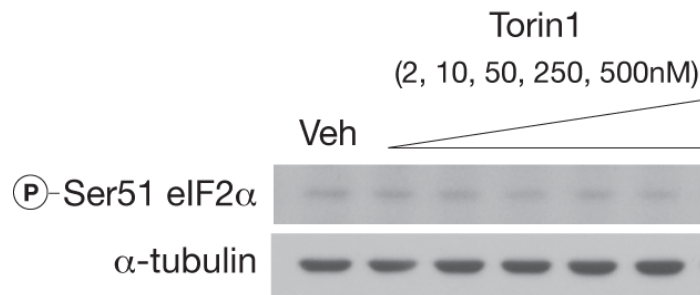


**Figure S5. mTOR inhibition does not affect eIF2 alpha phosphorylation.**

MEFs (p53<sup>-/-</sup>) were treated with vehicle (DMSO) or increasing concentrations of Torin1 for 1 h and then analyzed by immunoblotting for the indicated proteins and phosphorylation states.

## Supplemental References

1. Reichling, L. J., Lebakken, C. S., Riddle, S. M., Vedvik, K. L., Robers, M. B., Kopp, L. M., Bruinsma, R., and Vogel, K. W. (2008) *J Biomol Screen* **13**, 238-244